

Fabrication of C/SiC composites by combining liquid infiltration process and spark plasma sintering technique

Alba Centeno¹, Victoria G. Rocha², Amparo Borrell³, Clara Blanco¹, Adolfo Fernández^{2,3*}

¹Instituto Nacional del Carbón (INCAR-CSIC), Apartado 73, 33080, Oviedo, Spain

²ITMA Materials Technology, Parque Tecnológico de Asturias, 33428, Llanera, Spain

³Centro de Investigación en Nanomateriales y Nanotecnología (CINN) (CSIC - Universidad de Oviedo - Principado de Asturias), Parque Tecnológico de Asturias, 33428 Llanera, Spain

*Corresponding author. Address: ITMA Materials Technology, Parque Tecnológico de Asturias, 33428 Llanera (Asturias), Spain. Tel.: +34 985 980 058; Fax: +34 985 265 574. E-mail address: a.fernandez@itma.es (A. Fernández).

Abstract

Carbon fibre-reinforced silicon carbide composites (C-SiC) were fabricated combining, for the first time, a liquid infiltration process (LI) of a mesophase pitch doped with silicon carbide nanoparticles followed by reactive liquid silicon infiltration using Spark Plasma Sintering technique (SPS). A graphitization step was applied in order to improve the effectiveness of the processing. Up to three different morphologies of SiC particles were identified with a noticeable influence on the preliminary oxidation tests carried out. The presence of SiC nanoparticles added to the carbon matrix affects the morphology of

the SiC obtained by in-situ reaction of silicon and carbon during the LI process by SPS and it leads to an improvement of the material oxidation resistance. The results show that SPS is a promising method to develop C-SiC composites in a short time and with a high efficiency in the liquid silicon infiltration process.

Keywords: A. Sintering; B. C/SiC composites; B. Microstructure; Liquid infiltration process

1. Introduction

There are numerous alternatives concerning the fabrication of carbon fibre-reinforced silicon carbide composites (C-SiC). Chemical Vapor Infiltration (CVI) and Liquid Silicon Infiltration (LSI) of porous carbon fibre preform are the most universal methods used to produce C-SiC composites [1-3]. In the first one, different silicon sources can be used, such as mixtures of $(\text{CH}_3)\text{SiCl}_3/\text{H}_2$ or $(\text{C}_2\text{H}_5)\text{SiCl}_3/\text{H}_2$ and the processing takes up to several weeks due to the number of cycles which are necessary to apply in order to achieve high density materials [1]. Therefore, many efforts have been made to reduce the manufacturing time [4-6]. The processing by LSI consists on the infiltration of a porous carbon preform with molten silicon using a conventional furnace. Carbon and silicon react to form SiC at temperatures in the range of 1450-1650 °C and dwell time between 1-3h under vacuum [4]. This process leads to the development of C-SiC composites with lower component fabrication time and therefore reduced component costs [7,8].

The motivation of this work is to study new alternative methods to developed C-SiC composites decreasing the processing time. Spark Plasma Sintering (SPS) is

proposed as an easy and fast technique to produce C-SiC composites by reactive liquid silicon infiltration combined with Liquid Infiltration process (LI).

SPS, also known as field assisted sintering technique (FAST), is a sintering technique widely used in the processing of ceramic materials which can consolidate powder compacts applying an on-off dc electric pulse under uniaxial pressure [9]. This technique can operate at heating rates of the order of hundred degrees per minute, reaching high temperatures in a very short time and leading to dense materials after total processing duration just in the order of few minutes [10].

In this work, C-SiC composites are fabricated for first time by combining LI of a commercial mesophase pitch doped with silicon carbide nanoparticles followed by LSI using SPS technique.

2. Experimental procedure

The processing of the C-SiC composites consisted of two steps. The first step involved the liquid infiltration of a commercial mesophase pitch (supplied by Mitsubishi Gas Chemical) into a porous 2D twill weave PAN-based carbon fibre preform (supplied by SGL Carbon Group, Germany) leaving to the development of the undoped composite which will be used for comparison purposes. The infiltration process, widely used in the processing of carbon/carbon composites was carried out at 350 °C during 3h under nitrogen pressure of 0.5 MPa [11]. The materials obtained were carbonised at 1000 °C. Up to three infiltration/carbonisation cycles were applied (U-composite-C). Finally, the materials were graphitised at 2400 °C (U-composite-G). The corresponding doped material was obtained through the infiltration of the mesophase pitch doped with silicon carbide nanoparticles and labeled as SiC-composite-C and SiC-

composite-G for the carbonized and graphitised composites respectively. The doped matrix precursor was obtained previously by mixing 15 wt.% of SiC nanoparticles (45-50 nm, supplied by Sigma Aldrich) with the mesophase pitch at 350 °C during 2h, 300 rpm and nitrogen pressure of 0.2 MPa, using a similar procedure to that described in ref. [11]. The second step consisted on the Liquid Silicon Infiltration of the previous materials by SPS. The materials were placed into a graphite die, with an inner diameter of 20 mm, and covered with Si powder (supply by Sigma Aldrich). Then, they were sealed and introduced in a SPS Apparatus HP D 25/1 (FCT Systeme, Germany). The treatment was performed under vacuum (10^{-1} mbar) and applying at uniaxial pressure of 16 MPa from room temperature up to the end of the cycle. The applied heating rate was 50 °C min^{-1} up to 1000 °C followed by 25 °C min^{-1} up to the final temperature (1250-1500 °C). The dwell time at maximum temperature was 30 min. The whole time of the SPS process was around 1h. The materials were labeled as U-SPS and SiC-SPS.

The composites obtained were characterized attending to their microstructure by Scanning Electron Microscopy (SEM) and optical microscopy inspection. The bulk density was determined from the weight and geometry of the specimens. The open and close porosities were determined by Archimedes method and helium pycnometry respectively. Mercury intrusion porosimetry was carried out on carbonized and graphitized materials prior to LSI by SPS in order to study the pore size distribution in the preform. The measurements were carried out with Micrometris Autopore IV 9500 on specimens of 20 mm x 20 mm x 5 mm. SiC content of the composites was analyzed as follows. The minor free silicon was firstly removed by dissolving the composite in a mixture of hydrofluoric and nitric acid at 40 °C; the free carbon content was subsequently measured by thermal gravimetric analysis (TGA) at 700 °C under flowing air atmosphere; consequently, the remaining SiC content was calculated. In order to

evaluate their oxidation resistance, specimens $5 \times 5 \times 5 \text{ mm}^3$ in size, were placed in a thermogravimetric analyzer TGA CSI Instruments especially designed for testing samples up to 2 cm^3 . The installation also contains an electrobalance, with a detectable variation in mass of $0.1 \text{ }\mu\text{g}$, which continuously measures the weight of the sample, which is suspended in a platinum basket. A heating rate of $10 \text{ }^\circ\text{C min}^{-1}$ up to $900 \text{ }^\circ\text{C}$ was applied under N_2 flowing. Isothermal oxidation tests were carried out at $900 \text{ }^\circ\text{C}$ under air atmosphere.

3. Results and Discussion

After three pitch infiltration/carbonisation cycles, the initial porosity of the preforms (40 vol.%, entirely open) was reduced up to 13 vol.% (10 vol.% of open porosity and 3 vol.% of close porosity) for both composites, U-composite-C and SiC-composite-C and the initial bulk density was increased from 1.0 g cm^{-3} up to 1.54 g cm^{-3} and 1.58 g cm^{-3} , respectively (Table 1). After the pitch infiltration/carbonization cycles, part of the remaining porosity is close (3 vol.%) In order to facilitate the subsequent Liquid Silicon Infiltration by SPS, a graphitization treatment was applied previously with the aim to open the close porosity and to facilitate the access of Si. After this thermal treatment, the open porosity increased up to 17 vol.% and no close porosity was measured. Moreover, it is expected that the graphitization treatment also contributes to increase the thermal conductivity of the composite and improves its oxidation resistance [12-14].

Figure 1 shows the evolution of pore size distribution, obtained by Hg porosimetry, with the number of infiltration/carbonization cycles applied. The curve of the initial preform shows two distinct parts with limit $\sim 20 \text{ }\mu\text{m}$. The application of the first cycle produced a strong decrease of the porosity $< 20 \text{ }\mu\text{m}$, also confirmed by optical

microscopy studies (Figure 1a). The application of consecutive infiltration cycles produced a progress decrease of the large porous ($>20\ \mu\text{m}$). Optical microscopy studies confirm these tendencies. Figure 1b shows that the cracks, produced during the thermal treatments, are filled with matrix. After the third LI cycle the material was graphitized. During graphitization, the matrix undergoes a strong contraction and the different contractions produced between fibre and matrix cause cracking and porosity in the material. This translates into an increase in open porosity as a consequence of the opening of closed porosity. This increase was reflected in the mercury porosimetry curves (Figure 1), showing a slight increase in porosity with size lower than $20\ \mu\text{m}$. The same tendencies were observed for both, undoped and SiC-doped composites.

Optical microscopy inspection shows that the optical texture of the mesophase pitch matrix is affected by the presence of SiC nanoparticles, changing from domains to mosaics. It can be distinguished the mosaic optical texture (Figure 2a, position M) in areas where the SiC forms agglomerates specially close to the intersection of the bundles of fibres. SiC particles are usually in the range of sub-micron sizes and agglomerates are lower than $5\ \mu\text{m}$. On the other hand, a texture of domains, typical of the mesophase pitch, is observed in those areas where the dopant content is lower or its distribution is more homogeneous (Figure 2a, position D).

The Si-infiltration tests by SPS method were performed at different temperatures, from 1250 to $1500\ ^\circ\text{C}$ and dwell times of $30\ \text{min}$. The best results were obtained at 1400 - $1450\ ^\circ\text{C}$. When the melting point of silicon ($1410\ ^\circ\text{C}$) is reached, silicon rapidly infiltrates into the preform through cracks and microdelaminations produced during the previous thermal treatments. The combination of heating and pressure applied facilitates the liquid silicon diffusion. Figure 3a shows the high efficiency achieved in the infiltration process, being noticeable the high densification

achieved in the composite. The porosity was reduced to values as low as 5 vol.% (entirely open) and the corresponding bulk density was 1.8 and 2.0 gcm⁻³ for U-SPS and SiC-SPS, respectively. Microscopy inspection of both composites demonstrates that the matrix phase obtained by LSI through SPS technique corresponds mainly to a ceramic matrix of SiC (~12.0 wt.% of SiC). Only in those areas where there are big pores, residual silicon (~4.0 wt.% of Si) is observed in the centre and SiC carbide is only formed at the edges of the pores as usually occurs [15]. The observations show that silicon had reacted preferentially with carbon matrix, introduced during the previous LI process, to form silicon carbide and avoiding the damage of fibres (Figure 3b). As a consequence of the different carbon textures present in the materials already discussed in Figure 2 (domains texture in U-composite and both, domains and mosaic texture, in SiC-composite), the silicon carbide formed by in-situ reaction with these different textures of matrix during the LSI process shows different morphologies influenced by the carbon matrix from which it comes from. In the case of SiC-SPS composite three different SiC morphologies are expected: (1) the SiC nanoparticles added to the mesophase pitch during the LI process, (2) the SiC formed by reaction with the mosaic texture of carbon matrix and (3) the SiC formed by reaction with the domains texture. In the case of the U-SPS composite since only domains texture carbon matrix is present thus only one morphology of silicon carbide is expected. Due to these different morphologies of SiC it is predictable that each type of SiC particles will have different contribution to the oxidation behavior of the material as result of their own morphology and size. Thus, preliminary oxidation tests of the C-SiC composites, U-SPS and SiC-SPS, were carried out. The SiC-SPS composite shows lower oxidation rate than U-SPS as it can be concluded from the lower slope of the oxidation curve (Figure 4). The oxidation profile reveals the influence of the type of silicon carbide and its content on

the oxidation resistance of the material. Moreover, the residual weight is 15% higher that cannot only be explained by the presence of added SiC nanoparticles as its content is <3 wt.% in the whole material. This difference is also due to a higher carbon residual content after oxidation experiment in the SiC-SPS material. In the photograph of the SiC-SPS composite shown in Figure 4, it can be appreciated that the composite preserve its whole structure after the oxidation test. Therefore, this result confirms the protection of the carbon fibres by silicon carbide formed during LSI process applied by SPS method.

4. Conclusions

The efficiency of the SPS technique applied to liquid silicon infiltration and subsequent C-SiC composite preparation has been demonstrated for the first time. This is a very promising method for fast processing of C-SiC composite materials, considering the high heating rates that can be applied by this technique. The introduction of SiC nanoparticles during pitch infiltration influences the characteristics of SiC developed during LSI process and leads to an enhancement of the oxidation resistance of the composite material.

Acknowledgements

This work has been performed within the framework of the Integrated European Project “ExtreMat” (NMP-CT-2004-500253) and IP-NANOKER (NMP3-CT-2005-515784)with financial support by the European Community and the Spanish Education Ministry (Programa Nacional de Cooperación Internacional de Ciencia y Tecnología, Acciones Complementarias, MAT2004-22787-E). A. Borrell acknowledges the Spanish

Ministry of Science and Innovation for her FPI Ph.D. grant BES-2007-15033. Authors want to thank Belén González (INCAR-CSIC) for the TGA measurements.

References

- [1] P. Morgan, Carbon fibers and their composites. CRC Press, Taylor and Francis Group, LLC, 2005.
- [2] Q. Zhou, S. Dong, Y. Ding, Z. Wang, Z. Huang, D. Jiang, Three-dimensional carbon fiber-reinforced silicon carbide matrix composites by vapor silicon infiltration, *Ceram. Inter.* 35 (2009) 2161-2169.
- [3] J.C. Margiotta, D. Zhang, D.C. Nagle, Microstructural evolution during silicon carbide (SiC) formation by liquid silicon infiltration using optical microscopy, *Int. J. Refrac. Met. Hard Mater.* 28 (2010) 191-197.
- [4] J.C. Cavalier, A. Lacombe, J.M. Rouges, In developments in the science and technology of composite material, Elsevier, London, 1989, pp. 99-110.
- [5] P. Sangsuwan, J.A. Orejas, J.E. Gatica, S.N. Tewari, M. Singh, Reaction-Bonded Silicon Carbide by Reactive Infiltration, *Ind. Eng. Chem. Res.* 40 (2001) 5191-5198.
- [6] A.S. Mukasyan, J.D.E. White, Electrically induced liquid infiltration for the synthesis of carbon/carbon-silicon carbide composite, *Ceram. Inter.* 35 (2009) 3291-3299.
- [7] M. Bahraini, J.M. Molina, M. Kida, L. Weber, J. Narciso, A. Mortensen, Measuring and tailoring capillary forces during liquid metal infiltration, *Current Opinion Solid State Mater. Sci.* 9 (2005) 196-201.

- [8] Y. Xu, Y. Zhang, L. Cheng, L. Zhang, J. Lou, J. Zhang, Preparation and friction behavior of carbon fiber reinforced silicon carbide matrix composites, *Ceram. Inter.* 33 (2007) 439-445.
- [9] R.G. Joanna, Z. Antonios, Sintering activation by external electrical field, *Mater. Sci. Eng. A.* 287 (2000) 171–177.
- [10] Y. Wang, Z. Fu, Study of temperature field in spark plasma sintering. *Mater. Sci. Eng. B.* 90 (2002) 34-37.
- [11] A. Centeno, R. Santamaría, M. Granda, R. Menéndez, C. Blanco, Development of titanium-doped carbon/carbon composites, *J. Mater. Sci.* 44 (2009) 2525-2532.
- [12] G. Amirthan, A. Udayakumar, M. Balasubramanian, Thermal conductivity studies on Si/SiC ceramic composites, *Ceram. Inter.* 37 (2011) 423-426.
- [13] H. Li, L. Zhang, L. Cheng, Y. Wang, Fabrication of 2D C/ZrC-SiC composite and its structural evolution under high-temperature treatment up to 1800 °C, *Ceram. Inter.* 35 (2009) 2831-2836.
- [14] S. Li, X. Chen, Z. Chen, The effect of high temperature heat-treatment on the strength of C/C to C/C-SiC joints, *Carbon* 48 (2010) 3042-3049.
- [15] J. Schulte-Fischedick, A. Zern, J. Mayer, M. Rühle, M. Friess, W. Krenkel, M. Kochendörfer, The morphology of silicon carbide in C/C–SiC composites, *Mater. Sci. Eng. A.* 332 (2002) 146-152.

Table Captions:

Table 1. Physical properties of composites

Figure Captions:

Figure 1. Pore size distribution curves of composites. Optical micrographs of SiC-composite with: (a) one and (b) three liquid infiltration/carbonization cycles.

Figure 2. Optical micrographs: (a) SiC-composite-C and (b) SiC-SPS.

Figure 3. SEM micrographs corresponding with SiC-SPS composite.

Figure 4. Oxidation behaviour of U-SPS and SiC-SPS composites at 900 °C. Photograph of SiC-SPS after oxidation test.

Figure 1
[Click here to download high resolution image](#)

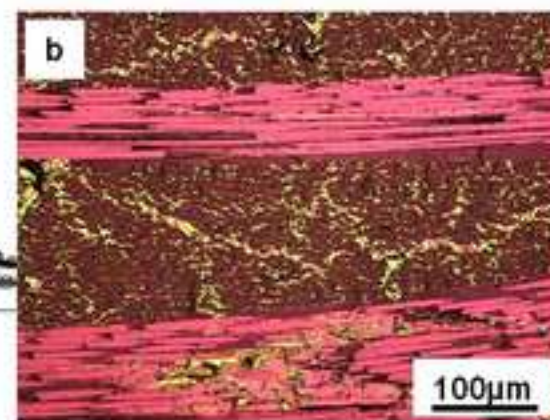
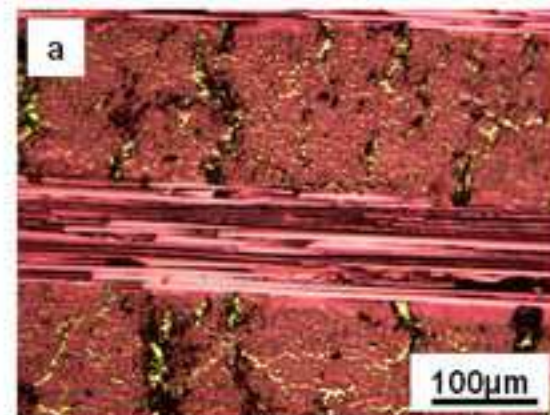
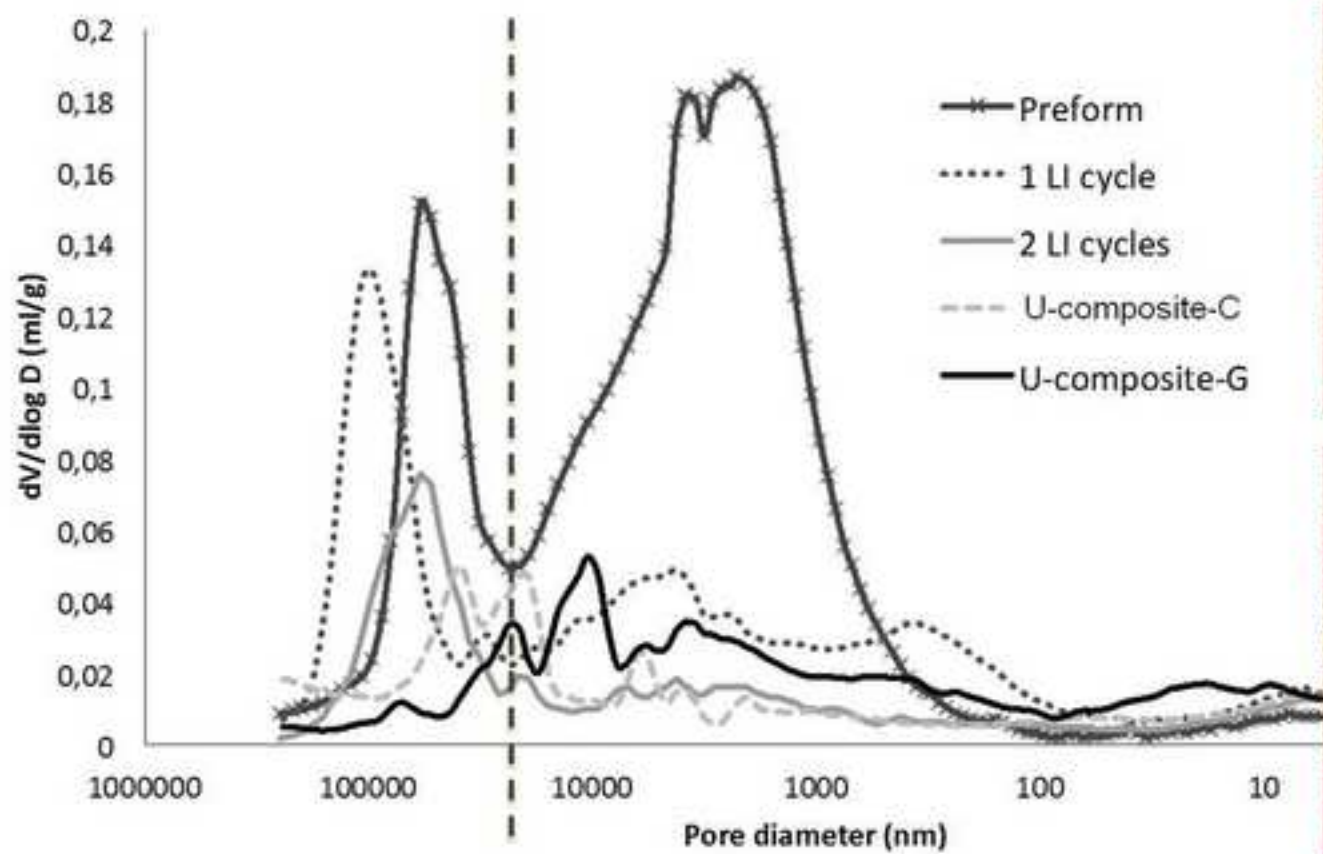


Figure 2
[Click here to download high resolution image](#)

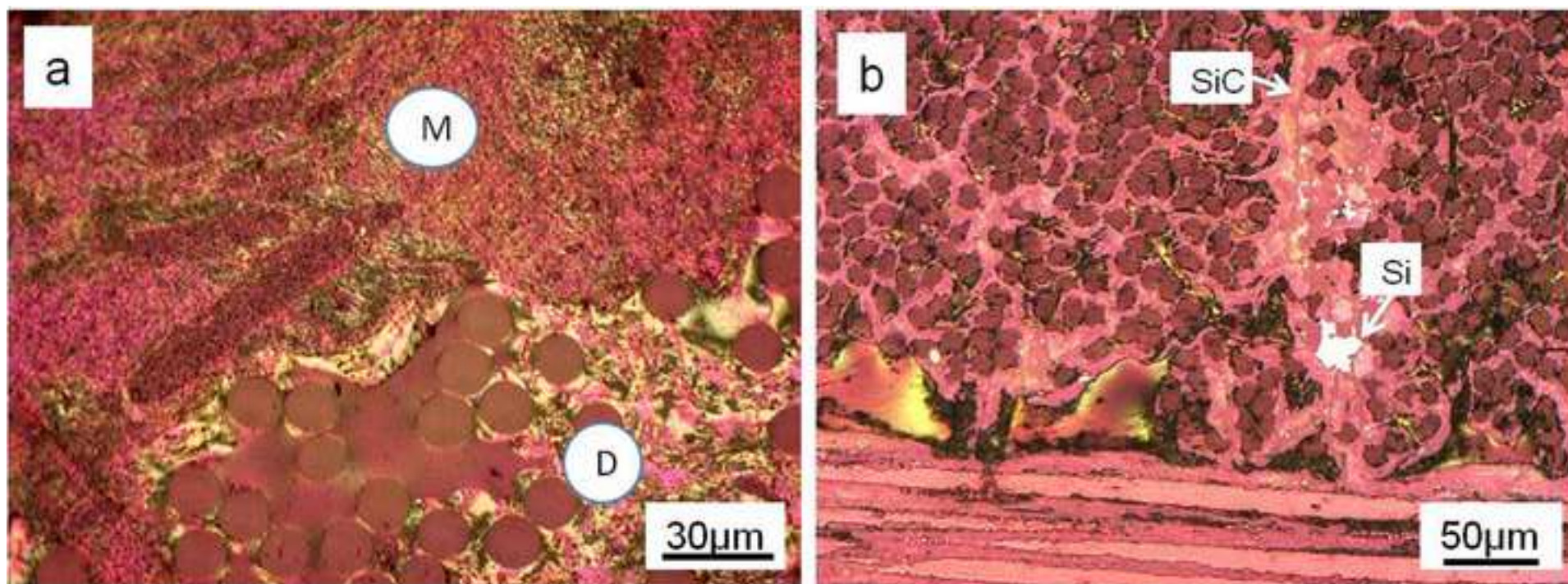


Figure 3
[Click here to download high resolution image](#)

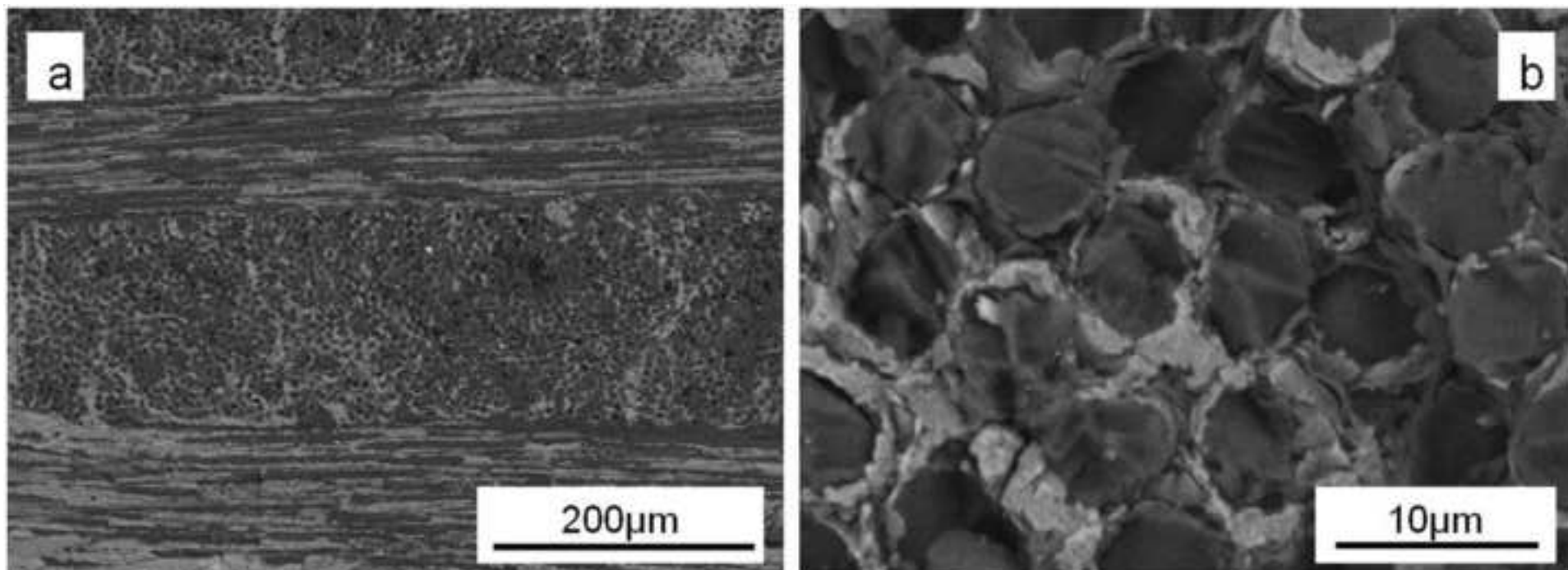


Figure 4
[Click here to download high resolution image](#)

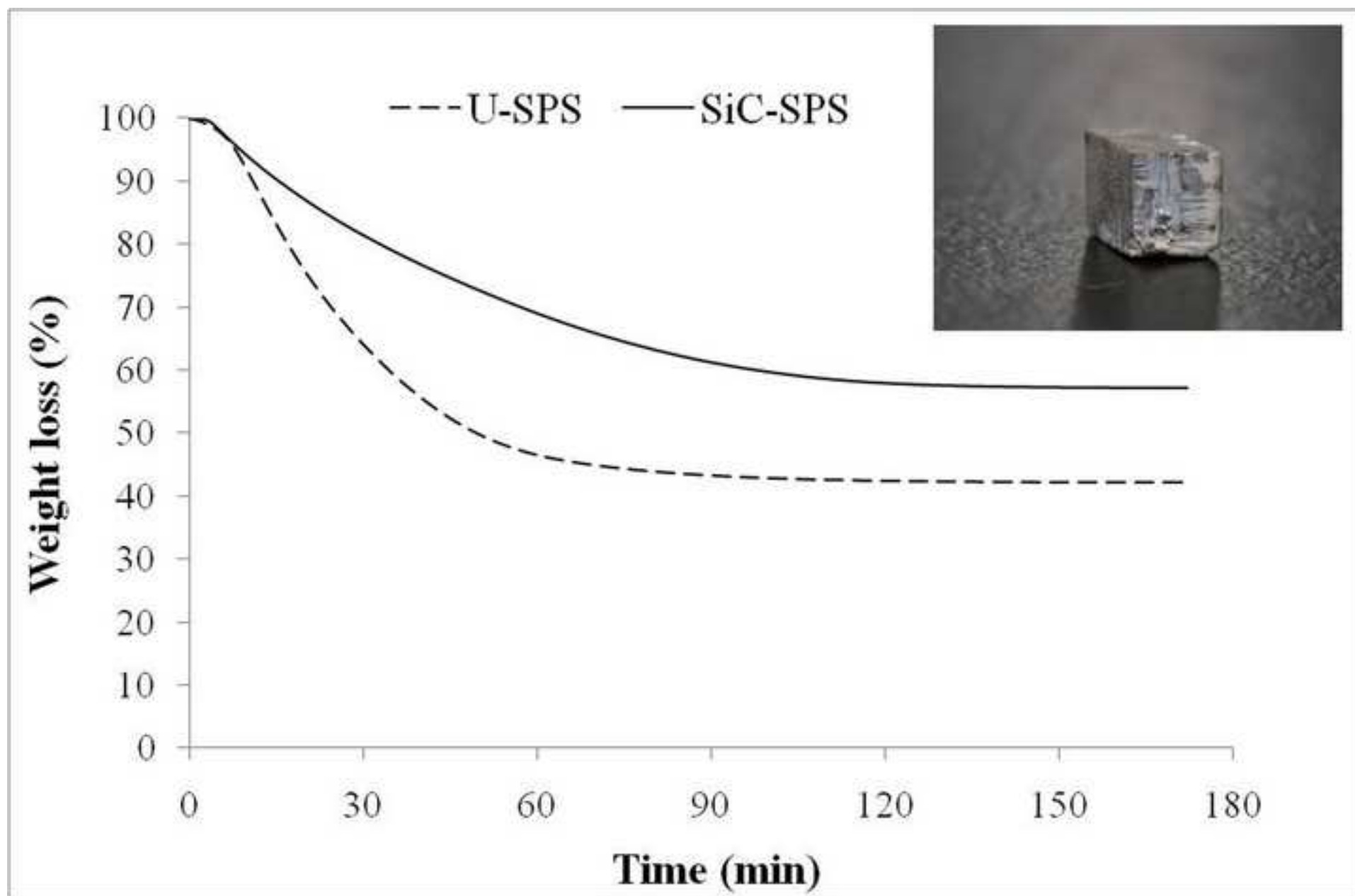


Table 1

MATERIAL	Open porosity (vol.%)	Close porosity (vol.%)	Density (g/cc)	SiC content (wt.%)	Free Si content (wt.%)
Preform	40	0	1	0	0
U-composite-C	10	3	1.54	0	0
SiC-composite-C	10	3	1.58	2.6	0
U-composite-G	17	0	1.57	0	0
SiC-composite-G	16	0	1.60	2.9	0
U-SPS	5	0	1.8	11.9	4.0
SiC-SPS	5	0	2.0	12.2	4.3

Table 1. Properties of CC-SiC composites.